Polyhedron 82 (2014) 2–6

Contents lists available at ScienceDirect

Polyhedron

journal homepage: www.elsevier.com/locate/poly

Ni complexes of redox-active pincers with pendant H-bonding sites as precursors for hydrogen production electrocatalysis

Oana R. Luca [a], Steven J. Konezny [a,b], Glendon B. Hunsinger [c,1], Peter Müller [d], Michael K. Takase [a], Robert H. Crabtree [b,a,*]

[a] Department of Chemistry, Yale University, P.O. Box 208107, New Haven, CT 06520-8107, USA
[b] Energy Sciences Institute, Yale University, P.O. Box 27394, West Haven, CT 06516-7394, USA
[c] Department of Geology and Geophysics: Earth Systems Center for Stable Isotopic Studies, Yale University, 210 Whitney Ave., New Haven, CT 06511, USA
[d] Department of Chemistry, Massachusetts Institute of Technology, 77 Massachusetts Avenue, Cambridge, MA 02139, USA

ARTICLE INFO

Article history:
Received 18 October 2013
Accepted 4 December 2013
Available online 13 December 2013

Keywords:
Water reduction
Redox-active ligand
Solar fuels

ABSTRACT

We describe the synthesis and characterization of novel redox-active tridentate pincer ligands with pendant H-bonding sites. The corresponding Ni complexes exhibit complex redox behavior and are active precursors in hydrogen production electrocatalysis, a property potentially relevant to solar-to-fuel conversion. The electrochemistry of the corresponding Zn complexes was investigated to explore ligand participation in the observed redox chemistry.

1. Introduction

In the context of a proposed hydrogen economy, the development of methods to produce hydrogen have been of increased interest in recent years [1–3]. Nickel complexes have received attention, as they have been shown to efficiently effect the electrode-driven reduction of protons to hydrogen, a process of interest in industrial applications [4,5]. The reverse process, oxidation of hydrogen to protons and electrons has also been achieved [6]. The mechanistic understanding gained from this reversible, biomimetic process [7,8] has been used to harness reducing equivalents in the reduction of CO_2 to liquid fuels [9] Both organometallic [10] and coordination pincer complexes [11–13] are electrocatalysts for $2H^+ + 2e^- \rightarrow H_2$.

Incorporation of redox-active substructures within the ligand framework of a metal complex has proved to be an effective strategy to facilitate multielectron reactions [14]. These ligand-based electron-reservoirs [15] act as either electron acceptors or donors in catalytic processes, thus imparting new or enhanced reactivity in both chemical and electrochemical applications [11,14,16]. They hold interest in their potential ability to facilitate multielectron chemistry in inexpensive, first row metals that normally prefer 1e redox steps.

The main emphasis of this paper is the synthesis and characterization of two novel, potentially redox-active ligands, $\mathbf{N_{5*}}$ and $\mathbf{N_7}$, containing pendant base naphthyridine groups, together with Zn and Ni complexes both of $\mathbf{N_7}$ (Fig. 1) and of the known [14b] $\mathbf{N_5}$. A crystal structure verifies the ability of $\mathbf{N_5}$ to engage in hydrogen bonding with a Ni-bound aqua ligand. Analogous Zn and Ni complexes of $\mathbf{N_{5*}}$ proved too insoluble for detailed study but we retain the ligand synthesis here because we believe it will prove useful for the coordination chemistry community as an analogue of $\mathbf{N_5}$ that no longer has the ability to hydrogen bond to a metal-bound ligand because of the remote placement of the distal N atom. We report the reductive electrochemical behavior of the Zn and Ni complexes and their possible implications in catalysis. $\mathbf{N_5}$ and $\mathbf{N_7}$ can be considered doubly non-innocent in permitting ligand-based redox-activity as well as having pendant, potentially H-bonding sites. We therefore believe that all three ligands will prove useful in future.

2. Synthesis and characterization

2,2′:6′,2″-Terpyridines have been explored extensively [17] as ligands and more recently have also received attention in catalytic [18–20] and energy-relevant photoelectrochemical applications [21–23] such as tethering molecular catalysts onto semiconductor surfaces [24,25].

* Corresponding author at: Department of Chemistry, Yale University, P.O. Box 208107, New Haven, CT 06520-8107, USA.
E-mail address: robert.crabtree@yale.edu (R.H. Crabtree).
[1] Current address: NREL–National Bioenergy Center15013 Denver W. Parkway MS 3313, Golden, CO 80401, USA

0277-5387/$ - see front matter © 2013 Elsevier Ltd. All rights reserved.
http://dx.doi.org/10.1016/j.poly.2013.12.003

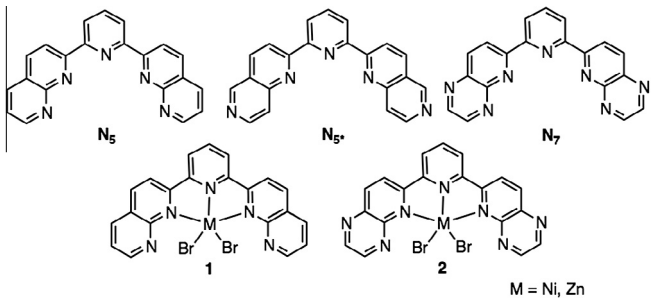

Fig. 1. Ligands $\mathbf{N_5}$, $\mathbf{N_{5*}}$, and $\mathbf{N_7}$ in their Zn ($\mathbf{1_{Zn}}$, $\mathbf{2_{Zn}}$) and Ni ($\mathbf{1_{Ni}}$, $\mathbf{2_{Ni}}$) complexes.

Fig. 1 (*left*) shows a known ligand of this type, $\mathbf{N_5}$, that was reported in 2005 along with its mononuclear Ru complex by Zong and Thummel [26]. This proved to be highly active for water oxidation, and although the role of the pendant N-atom of the naphthyridine remains a matter for discussion, the proposed mechanism may involve the active participation of the naphthyridine arm in the coordination and deprotonation of a bound water [27].

Boyer et al. [28] have investigated the water oxidation and water reduction activity of a series of mononuclear Ru complexes with a pyridine-2-(1,8-naphthyridine) ligand. The catalytic activity was highly dependent on whether the pendant basic sites were proximal or distal to the metal center. This prompted us to expand the polyaza ligand series with two new derivatives: $\mathbf{N_7}$ and $\mathbf{N_{5*}}$ (Fig. 1) to study their electrochemical properties to look for ligand-centered reduction.

The ligands were synthesized from commercially available starting materials *via* a Friedländer condensation of 2,6-diacetylpyridine and the corresponding nicotinamide (Fig. 2); their Ni(II) and Zn(II) complexes were then prepared by standard methods. (See Supporting information for details). The compounds showed limited solubility in both acetonitrile and water: in particular, the Zn and Ni derivatives of $\mathbf{N_{5*}}$ were too insoluble for detailed study and were therefore set aside. We retain the synthesis of the $\mathbf{N_{5*}}$ ligand in this report in case it may prove useful.

3. Electrochemistry of 1_{Zn} and 2_{Zn} showing redox activity of the ligands

The delocalized ligand framework was designed in the hope of promoting reductive ligand-based redox activity and the pendant N atoms were thought likely to favor both H-bonding and proton shuttling and thus facilitate catalytic proton reduction with H_2 formation. To probe this idea, we synthesized $\mathbf{1_{Zn}}$ and $\mathbf{2_{Zn}}$ and studied their electrochemical response in acetonitrile at a glassy C electrode. Interestingly, $\mathbf{1_{Zn}}$ did indeed show what we assign to a one-electron reduction process at −0.81 V vs. NHE (Fig. 3*left*) which we assign to the ligand as Zn is redox-inactive. A similar analysis for $\mathbf{2_{Zn}}$ showed two one-electron responses at −0.49 and −1.05 V versus NHE (Fig. 3 *right*). Although affected by solubility problems, the redox activity was clearly apparent. We cannot be certain that the complexes retain their structure in solution, although a 4-coordinate complex can be excluded because it would show an NMR spectrum.

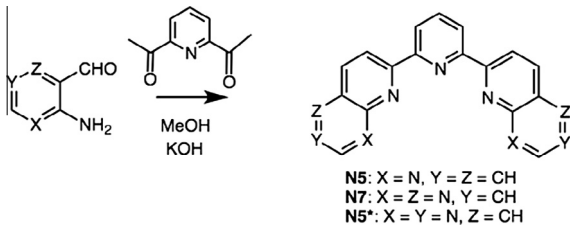

Fig. 2. Synthetic route to the **N5**, **N7** and **N5*** ligands.

The multielectron ligand redox behavior of $\mathbf{2_{Zn}}$ suggests that two reducing equivalents could be hosted within the ligand framework without reduction of the metal center. This is particularly interesting since the reduction of protons to hydrogen is a $2e^-$ process. Indeed, Wieghardt and coworkers [29] have reported catalytic alcohol oxidation by Zn complexes with redox-active ligands. Our Zn complexes were not catalytically active for water reduction, however, suggesting that Zn was not able to form the needed hydride intermediates; hydrides being better known for Ni than for Zn, we next studied the analogous Ni compounds.

4. Ni Electrochemistry

The Ni analogues of $\mathbf{1_{Zn}}$ and $\mathbf{2_{Zn}}$ have a quite different electrochemical response from the Zn complexes. $\mathbf{1_{Ni}}$ exhibits two reduction features at −0.87 V (broad, irreversible) and −1.48 V (Fig. 4 *left*) respectively. Given the pattern of electrochemical behavior of $\mathbf{1_{Zn}}$, the responses for $\mathbf{1_{Ni}}$ are likely due to a one-electron reduction of the ligand followed by a $Ni^{II} \rightarrow Ni^{I}$ metal-centered reduction. In contrast with these results, $\mathbf{1_{Ni}}$ showed an irreversible feature at −0.51 V versus NHE followed by a second reduction at −1.05 V versus NHE.

In order to pinpoint the potentials of the irreversible waves, we performed square-wave voltammetry (SWV). Using this technique we also attempted to assign the number of electrons for each of the observed transitions, by comparing the electrochemical response against a ferrocene standard SWV at the same concentration as the analyte under study. This analysis is of course contingent upon the diffusional coefficient of ferrocene being comparable with the diffusion coefficients of $\mathbf{1_{Ni}}$ and $\mathbf{2_{Ni}}$.

We see two $1e^-$ responses in Fig. 4 corresponding to $\mathbf{1_{Ni}}$ but a quite different behavior for $\mathbf{2_{Ni}}$, which shows a reduction feature assignable to a $2e^-$ event at −0.51 V. Since $\mathbf{2_{Zn}}$ had a reduction signal at −0.49 versus NHE, we believe the −0.51 V response of $\mathbf{2_{Ni}}$ corresponds to a combination of a $1e^-$ reduction of the ligand and a $1e^-$ reduction of the metal center at the same potential. This feature is then followed by a reduction akin to the second reduction feature of $\mathbf{2_{Zn}}$, which would correspond to a ligand centered event. However, we cannot exclude the possibility of complex adsorption on the electrode surface. This would bring some uncertainty to the interpretation of the number of electrons from square wave voltammetry.

In order to establish the structure of our Ni compounds, we attempted to crystallize $\mathbf{1_{Ni}}$ and $\mathbf{2_{Ni}}$ from water but were only able to obtain a crystal structure of $\mathbf{1_{Ni}}$ using a mixture of water/methanol (Fig. 5). The structure indicated the role of a pendant pyridine in moderately strong hydrogen bonding with an in-plane water molecule, the proton of which was located (O1···N1 = 2.767(6) A; O1–H–N1 = 150(8)°); the outer sphere O···Br distance indicates a rather weaker interaction (O2···Br2 = 3.188(4) A; O2–H–Br2 = 164(8)°) but the inner sphere distance (O1···Br1 = 3.42 A; O1–H–Br1 = 114(6)°) is constrained by the geometry. Ni(II) is notorious for showing 4-, 5- and 6- coordination depending on conditions so we do not attempt to define the coordination number in solution. A similar structure is expected to occur for $\mathbf{2_{Ni}}$ but X-ray-quality crystals could not be obtained in this case.

The crystal structure of Fig. 5 indicates that an in-plane water molecule is hydrogen-bonded to a naphthyridine side-arm of the $\mathbf{1_{Ni}}$ pincer ligand. This interaction may lower the pK_a of the remaining basic site, thus decreasing the likelihood of a second

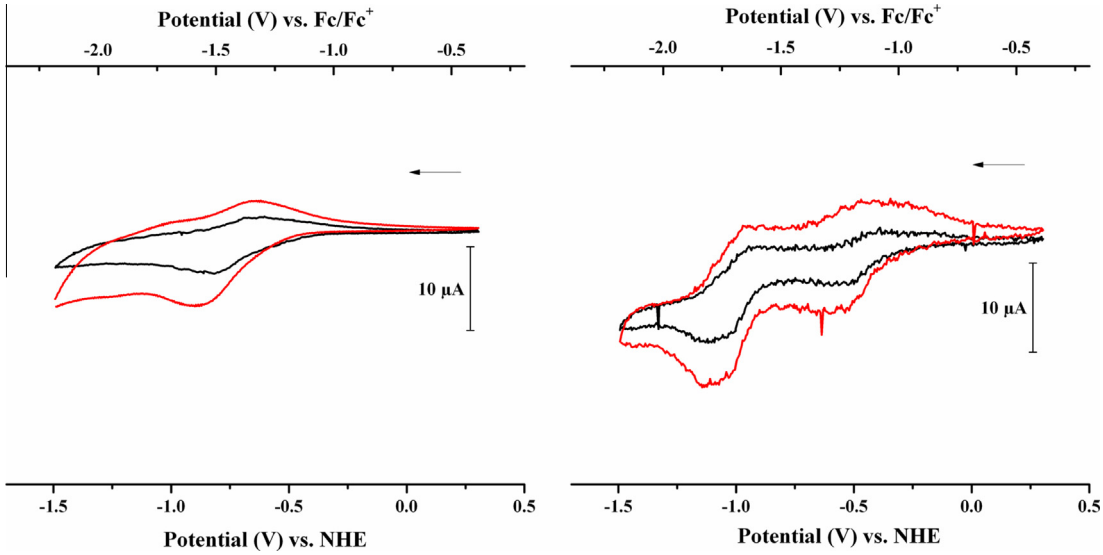

Fig. 3. *Left* Cyclic voltammogram of a 0.2 mM solution $\mathbf{1_{Zn}}$ in acetonitrile 0.1 M NBu_4BF_4 (black 50 mV/s, red: 100 mV/s). *Right* Cyclic voltammogram of a 0.2 mM solution $\mathbf{2_{Zn}}$ in acetonitrile 0.1 M NBu_4BF_4 (black 50 mV/s, red: 100 mV/s). (Color online.)

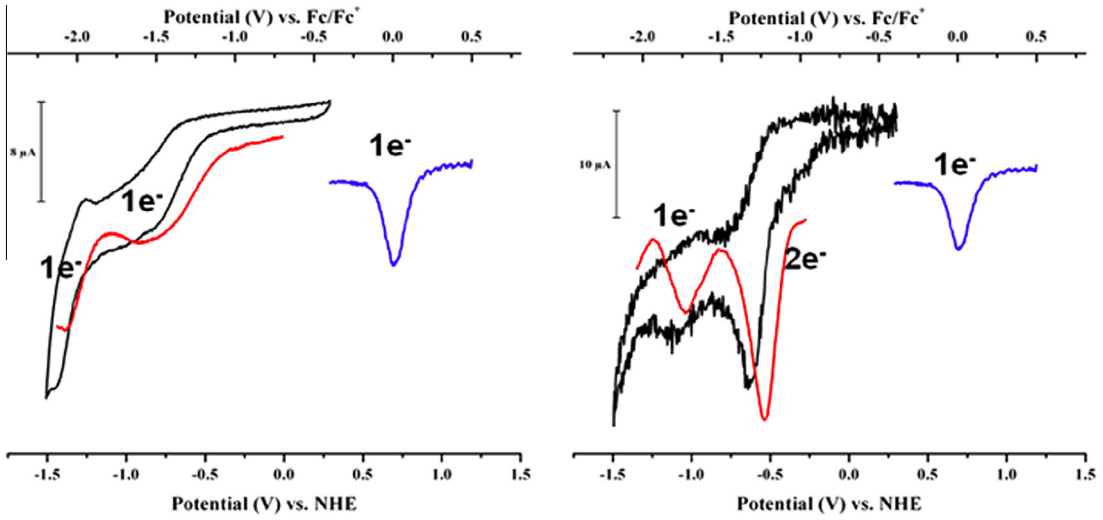

Fig. 4. *Left* Cyclic voltammogram of a 0.2 mM solution $\mathbf{1_{Ni}}$ in acetonitrile with 0.1 M NBu_4BF_4 (black 50 mV/s). Red: Square wave voltammetry of $\mathbf{1_{Ni}}$ (Square amplitude: 20 mV, Increment: 5 mV, Period: 5 ms, Width: 1 ms). *Right* Cyclic voltammogram of a 0.2 mM solution $\mathbf{2_{Ni}}$ in acetonitrile with 0.1 M NBu_4BF_4 (black 50 mV/s). Red: Square wave voltammetry of $\mathbf{1_{Ni}}$ (Square amplitude: 20 mV, Increment: 5 mV, Period: 5 ms, Width: 1 ms). The ferrocene response is shown in blue. (Right. Color online.)

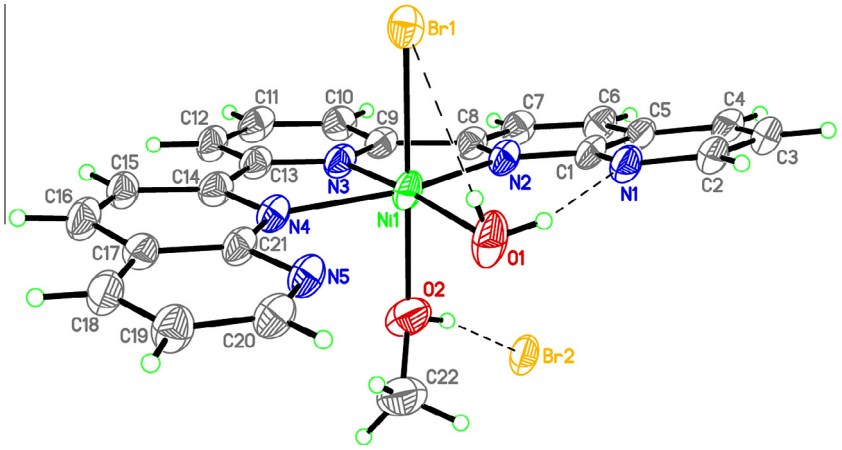

Fig. 5. Thermal ellipsoids at the 50% probability level for the crystal structure of $\mathbf{1_{Ni}}$ crystallized from water/methanol with the crystallographic labeling scheme.

Table 1
Number of turnovers (±3%) observed from quantitative headspace analysis H_2 measurements: mol H_2/mol catalyst after 30 min of electrolysis. The setup was a custom built two-cylinder 50 mL bulk electrolysis H-cell anode/cathode chamber separated by a coarse frit. The working electrode was a reticulated vitreous carbon electrode from Bioanalytical Systems MF-2077 referenced vs. Ag/AgCl (KCl_{sat}). The counter electrode was a 2.5 cm by 2.5 cm Pt mesh.

Conditions	Turnover number 1_{Ni}	Turnover number 2_{Ni}
pH 1 KCl/HCl −0.5 V vs. NHE	55	43
pH 4 phosphate 0.05 M −0.8 V vs. NHE	136	46
pH 7 phosphate 0.05 M −1.1 V vs. NHE	7.6	224

protonation event. Reduction to Ni(I) would be expected to increase the basicity of the N atoms, however. Density functional theory calculations at the UB3LYP/LACVP/6-311G* level [30,31] using optimized structures based on the crystal structure of **1_{Ni}** have been included in the SI (Fig. 5; Supporting information).

In order to test the comparative catalytic abilities of **1_{Ni}** and **2_{Ni}** for water reduction, we performed bulk electrolysis at three different different pH values with 4.5 μM catalyst loading and then calculated the number of turnovers observed after 30 min of electrolysis, after the necessary background subtractions (Table 1).

The pH dependence of catalysis differed for the two ligands, **N5** and **N7**. At pH 1, both catalyst precursors have similar turnover numbers at an applied overpotential of 440 mV (55 mol H_2/mol catalyst for **1_{Ni}** versus 46 mol H_2/mol catalyst **2_{Ni}**). **1_{Ni}** showed the highest turnover at pH 4, releasing 136 mol H_2/mol catalyst at 560 mV of applied overpotential, whereas **2_{Ni}** only showed a third of the activity under the same conditions: 46 mol H_2/mol catalyst. Surprisingly, **2_{Ni}** showed great activity at pH 7 with a turnover number of 224 mol H_2/mol catalyst compared to **1_{Ni}** where only a modest 7.6 turnovers were observed at 690 mV of applied overpotential. The Faradaic yields (Supplementary data) are strongly dependent on the conditions. For **1_{Ni}** they are adequate (80% ± 4%) at pH 1 in KCl/HCl, but much poorer at lower pH in phosphate buffers. For **2_{Ni}** they are similarly adequate at pH 1 and 7 but not at pH 4.

Heterogeneity problems can be misleading in catalysis if the catalyst precursor is converted to a heterogeneous catalyst during the reaction [32]. In the present case, we verified that the electrode, once rinsed and returned to a solution containing electrolyte alone with no Ni complex present, gave no current above background, so a catalytic deposit on the electrode is excluded. We cannot definitively exclude a nanoparticulate material being formed in solution, however.

5. Conclusion

We report the new **N_7** and **N_{5*}** ligand frameworks, designed to be redox active as well as possessing pendant H-bonding sites. Our results suggest that precatalyst **2_{Ni}** is indeed capable of accepting two electrons within the ligand framework, whereas compound **1_{Ni}** can only host one electron in this way. Moreover, precatalyst **2_{Ni}**, having a $2e^-$ redox-active ligand, has been shown to act as an active precursor for electrocatalytic water reduction under neutral conditions.

6. Experimental

6.1. General methods

All reagents were received from commercial sources and used without further purification unless otherwise specified. 4-amino-3-formyl-pyridine was purchased from Synthonix Inc. Solvents were dried by passage through a column of activated alumina followed by storage under dinitrogen. NMR spectra were recorded at room temperature on Bruker AMX-400 or 500 MHz spectrometers unless otherwise specified. Chemical shifts are reported with respect to residual internal protio solvent for ^1H and ^{13}C NMR spectra and to an external standard. Elemental analyses were performed by Robertson Microlit Inc.

Electrochemical data was recorded on a Pine Instruments AFCBP1 Bipotentiostat. Cyclic voltammograms in acetonitrile (0.1 M NBu_4BF_4) were collected at a glassy carbon working electrode (3 mm diameter, BASi) with a double junction BASi reference electrode (MF-2030 referenced versus NHE with ferrocene as external standard. Electrochemistry in acetonitrile was performed in 3 mL 0.1 M NBu_4BF_4 at 0.2 mM concentration of the respective analytes. All CVs were recorded after rigorous exclusion of air via Argon purge. Square wave voltammetry was performed in an identical setup to the cyclic voltammogram collection parameters (Square amplitude: 20 mV, Increment: 5 mV, Period: 5 ms, Width: 1 ms). Data workup was performed on OriginPro v8.0988 and AfterMath Data Organizer Version 1.2.3383.

Controlled potential headspace H_2 detection experiments were performed in a custom built two-cylinder 50 mL bulk electrolysis H cell anode/cathode chamber separated by a coarse frit. The working electrode was a reticulated vitreous carbon electrode from Bioanalytical Systems MF-2077 referenced versus Ag/AgCl (KCl_{sat}). Headspace H_2 detection was performed at the Yale Department of Geology on a calibrated mass spectrometer: dual inlet Thermo Finnegan MDT 253 and an air-tight bulk electrolysis H Cell equipped with a sampling port after 30 min of electrolyses. Prior to each experiment, the headspace and solution was sparged with He gas for ten minutes. 1 mL volumes of headspace gas were compressed in the bellows then opened to the mass spectrometer for analysis.

Acknowledgments

The work was supported as part of the Center for Electrocatalysis, Transport Phenomena, and Materials (CETM) for Innovative Energy Storage, an Energy Frontier Research Center funded by the U.S. Department of Energy, Office of Science, Office of Basic Energy Sciences under Award Number DE-SC00001055 (O.L. and RHC). We also thank Daryl Smith for the electrochemical cell design and Jesus Campos for experimental assistance.

Appendix A. Supplementary data

Supplementary data associated with this article can be found, in the online version, at http://dx.doi.org/10.1016/j.poly.2013.12.003.

References

[1] G.W. Crabtree, M.S. Dresselhaus, M.V. Buchanan, Phys. Today 57 (2004) 39.
[2] R. Crabtree, O. Luca, WO Patent 2,012,112,758, 2012.
[3] D. Das, T.N. Veziroğlu, Int. J. Hydrogen Energy 26 (2001) 13.
[4] M.L. Helm, M.P. Stewart, R.M. Bullock, M.R. DuBois, D.L. DuBois, Science 333 (2011) 863.
[5] E. Endoh, H. Otouma, T. Morimoto, Int. J. Hydrogen Energy 13 (1988) 207.
[6] M. Rakowski Dubois, D.L. Dubois, Acc. Chem. Res. 42 (2009) 1974.
[7] G.J. Kubas, Chem. Rev. 107 (2007) 4152.
[8] J.C. Fontecilla-Camps, A. Volbeda, C. Cavazza, Y. Nicolet, Chem. Rev. 107 (2007) 4273.
[9] E.E. Benson, C.P. Kubiak, A.J. Sathrum, J.M. Smieja, Chem. Soc. Rev. 38 (2009) 89.
[10] O.R. Luca, J.D. Blakemore, S.J. Konezny, J.M. Praetorius, T.J. Schmeier, G.B. Hunsinger, V.S. Batista, G.W. Brudvig, N. Hazari, R.H. Crabtree, Inorg. Chem. 51 (2012) 8704.
[11] O.R. Luca, S.J. Konezny, J.D. Blakemore, D.M. Colosi, S. Saha, G.W. Brudvig, V.S. Batista, R.H. Crabtree, New J. Chem. 36 (2012) 1149.

[12] O.R. Luca, S.J. Konezny, E.K. Paulson, F. Habib, K.M. Luthy, M. Murugesu, R.H. Crabtree, V.S. Batista, Dalton Trans. 42 (2013) 8802.
[13] B.D. Stubbert, J.C. Peters, H.B. Gray, J. Am. Chem. Soc. 133 (2011) 18070.
[14] (a) O.R. Luca, R.H. Crabtree, Chem. Soc. Rev. 42 (2013) 1440;
(b) R.P. Thummel, Inorg. Chem. 26 (1986) 2524.
[15] O.R. Luca, T. Wang, S.J. Konezny, V.S. Batista, R.H. Crabtree, New J. Chem. 35 (2011) 998.
[16] O.R. Luca, D.L. Wang, M.K. Takase, R.H. Crabtree, New J. Chem. 37 (2013) 3402.
[17] A.M.W. Cargill, Coord. Chem. Rev. 160 (1997) 1.
[18] J. Limburg, G.W. Brudvig, R.H. Crabtree, J. Am. Chem. Soc. 119 (1997) 2761.
[19] H. Chen, J.W. Faller, R.H. Crabtree, G.W. Brudvig, J. Am. Chem. Soc. 126 (2004) 7345.
[20] S. Das, C.D. Incarvito, R.H. Crabtree, G.W. Brudvig, Science 312 (2006) 1941.
[21] J.J. Concepcion, J.W. Jurss, M.K. Brennaman, P.G. Hoertz, A.O.v.T Patrocinio, N.Y. Murakami Iha, J.L. Templeton, T.J. Meyer, Acc. Chem. Res. 42 (2009) 1954.
[22] A. Llobet, P. Doppelt, T.J. Meyer, Inorg. Chem. 27 (1988) 514.
[23] H. Hofmeier, U.S. Schubert, Chem. Soc. Rev. 33 (2004) 373.
[24] W.R. McNamara, R.C. Snoeberger, G. Li, J.M. Schleicher, C.W. Cady, M. Poyatos, C.A. Schmuttenmaer, R.H. Crabtree, G.W. Brudvig, V.S. Batista, J. Am. Chem. Soc. 130 (2008) 14329.
[25] J.D. Sokolow, E. Trzop, Y. Chen, J. Tang, L.J. Allen, R.H. Crabtree, J.B. Benedict, P. Coppens, J. Am. Chem. Soc. 134 (2012) 11695.
[26] R. Zong, R.P. Thummel, J. Am. Chem. Soc. 127 (2005) 12802.
[27] Y.M. Badiei, D.E. Polyansky, J.T. Muckerman, D.J. Szalda, R. Haberdar, R. Zong, R.P. Thummel, E. Fujita, Inorg. Chem. 52 (2013) 8845.
[28] J.L. Boyer, D.E. Polyansky, D.J. Szalda, R. Zong, R.P. Thummel, E. Fujita, Angew. Chem., Int. Ed. 50 (2011) 12600.
[29] P. Chaudhuri, M. Hess, J. Müller, K. Hildenbrand, E. Bill, T. Weyhermüller, K. Wieghardt, J. Am. Chem. Soc. 121 (1999) 9599.
[30] S.J. Konezny, M.D. Doherty, O.R. Luca, R.H. Crabtree, G.L. Soloveichik, V.S. Batista, J. Phys. Chem. C 116 (2012) 6349.
[31] Jaguar, version 7.9, Schrodinger, LLC, New York, NY, 2011.
[32] R.H. Crabtree, Chem Rev. 112 (2012) 1536.